DINAME 2017 - Proceedings of the XVII International Symposium on Dynamic Problems of Mechanics
A. T. Fleury, D. A. Rade, P. R. G. Kurka (Editors), ABCM, São Sebastião, SP, Brazil, March 5-10, 2017

Overhead crane sliding mode control with saturation and variable setpoint

S. L. H. Cavallaro[1], **D. C. Donha**[1]

[1] Escola Politécnica da Universidade de São Paulo, Av. Prof. Luciano Gualberto, 380, São Paulo, Brazil, cavallaro.silvio@gmail.com, decdonha@usp.br

Abstract: In this article a non-linear and robust controller is synthetized to control a sub-actuated overhead crane, aiming at sway angle amplitude and frequency reduction by penalizing the trolley accuracy and payload mass travel time. Combining sliding mode controller with saturation and variable setpoint was synthesized to ensure performance requirements in usual applications. The closed loop system performance proved to be satisfactory, even considering parametric uncertainties. The trolley reaches its destination in a fast way, without harmful oscillation of the payload mass.

Keywords: Overhead crane; modeling; control; sliding mode; saturation; variable setpoint

INTRODUCTION

An overhead crane basically consists of a cart or trolley, which moves along a rail, transporting payloads by a cable. These cranes are extensively applied in industrial fields due to their low cost, easy assembly and maintenance (Nazemizadeh, 2013). They are suitable for several purposes, mainly related to load transportation from a position to another one, optimizing the available space inside industrial sheds, ports, among other places. Overhead cranes had become an appealing task in the fields of dynamic and control, aiming payload mass travel time optimization, trolley accuracy, sway angle amplitude and frequency reduction (Nazemizadeh, 2013). Even though, because of commitment relationship between performance objectives, it's necessary to choose between the optimization of the trolley accuracy or the sway angle reduction. In the past decades, techniques of oscillation frequency and sway angle amplitude suppression were prioritized against the payload mass travel time and trolley accuracy (Park *et al., 2007)*. This article also pursues these goals through the synthetizes of a non-linear control.

PROBLEM ADDRESED

An overhead crane consists basically of four elements: the trolley, which moves along a horizontal rail; the cable, which connects the trolley to the payload; the payload and the motor, which is responsible for moving the trolley. We model the overhead crane using two-degrees of freedom: the trolley horizontal movement x and the angle between the load and the vertical θ, called sway angle.

SIMPLIFYING ASSUMPTIONS

In order to reduce the problem complexity level, we adopted usual modeling simplifying assumptions as: the cable is considered as a rigid body, the trolley and the payload mass are considered as concentrated masses, the cable is inextensible and its mass is negligible, the electric circuit inductance is negligible and there are no electromagnetic losses on the electric motor, supposed to be a Direct Current (DC) motor.

SYSTEM DYNAMICS

Motor dynamics

The electric motor is a direct current (DC) controlled by armature current, which is represented by the following electric circuit (Bolton, 2004):

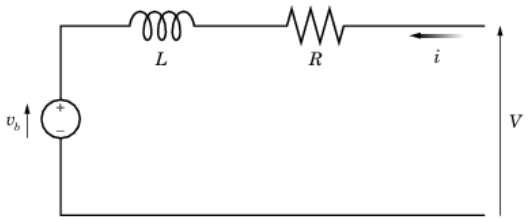

Figure 1 – DC motor electric circuit.

where R is the armature resistance, L is the armature inductance, v_b is the back electromotive force, i is the armature current and V is the voltage source. The following relationships are also assumed:

$$T = k_1 \cdot i \tag{1}$$

$$v_b = k_2 \cdot \omega \tag{2}$$

where T is the torque generated by the motor, k_1 is the torque constant, k_2 is the back electromotive force constant and ω is the motor angular speed. Considering that there are no electromagnetic losses on the DC motor, the mechanical power is equal to the power dissipated by the back electromotive force in the armature (Bolton, 2004). Therefore:

$$T \cdot \omega = v_b \cdot i \tag{3}$$

$$k_1 = k_2 = k \tag{4}$$

where k is the DC motor constant. Finally, applying the Ohm's law in the electric circuit shown in Fig. 1, we have:

$$T = \frac{k \cdot V}{R} - \frac{k^2 \cdot \omega}{R} \tag{5}$$

The force f applied in the car comes from the DC motor torque. Thus, the relation between the force and the voltage source can be derived as follows (Jafari *et al.*, 2014):

$$f = \frac{k \cdot V}{R \cdot r} - \frac{k^2 \cdot \dot{x}}{R \cdot r^2} \tag{6}$$

where $\dot{x}$ is the linear trolley velocity and r is the trolley wheel radius.

Overhead crane dynamics

We show an overhead crane physical model in Fig. 2, which includes a concentrated mass representing the trolley; a bar that connects the trolley to the payload mass, which is also represented as a concentrated mass.

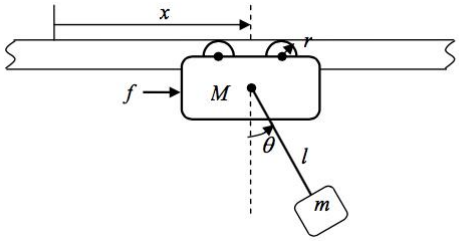

Figure 2 – Physical model of the overhead crane.

We derive the overhead crane equations of motion by Lagrange's Mechanics. The trolley kinetic energy T_1 and the payload kinetic energy T_2 are given as follows (Jafari *et al.*, 2014):

$$T_1 = \frac{1}{2} \cdot M \cdot \dot{x}^2 \tag{7}$$

$$T_2 = \frac{1}{2} \cdot m \cdot \left(\dot{x}^2 + l^2 \cdot \dot{\theta}^2 + 2 \cdot \dot{x} \cdot l \cdot \dot{\theta} \cdot \cos\theta \right) \tag{8}$$

where M is trolley mass, m is the payload mass, l is the cable length, θ is the sway angle, $\dot{\theta}$ is the sway angular velocity. The trolley and payload potential energy U_1 and U_2 can be derived as follows (Jafari *et al*., 2014):

$$U_1 = 0 \tag{9}$$

$$U_2 = -m \cdot g \cdot l \cdot \cos\theta \tag{10}$$

where g is the gravity acceleration. The Lagrange's function is given by (França and Matsumara, 2012):

$$L = T_1 + T_2 - V \tag{11}$$

The proposed system generalized forces are (Jafari *et al*., 2014):

$$Q_x = f \tag{12}$$

$$Q_\theta = 0 \tag{13}$$

$$Q_{x,lost} = B_{eq} \cdot \dot{x} \tag{14}$$

$$Q_{\theta,lost} = B_p \cdot \dot{\theta} \tag{15}$$

where Q_x is the generalized force exerted in the generalized coordinate x, Q_θ is the generalized force exerted in the generalized coordinate θ, $Q_{x,lost}$ is the dissipation force exerted in the generalized coordinate x, $Q_{\theta,lost}$ is the dissipation force exerted in the generalized coordinate θ, B_{eq} is the equivalent viscous damping coefficient and B_p is the cable viscous damping coefficient. Finally, applying the Lagrange's principle together with Eq. (6), we have:

$$\left(M + m\right) \cdot \ddot{x} + m \cdot l \cdot \left(\ddot{\theta} \cdot \cos\theta - \dot{\theta}^2 \cdot \sin\theta \right) = f - B_{eq} \cdot \dot{x} \tag{16}$$

$$m \cdot l \cdot \left(\ddot{x} \cdot \cos\theta + l \cdot \ddot{\theta} + g \cdot \sin\theta \right) = -B_p \cdot \dot{\theta} \tag{17}$$

where $\ddot{x}$ is the trolley linear acceleration and $\ddot{\theta}$ is the sway angular acceleration.

STATE VARIABLES AND OUTPUTS

The state vector and the system output are the following:

$$x^T = \begin{bmatrix} x & \dot{x} & \theta & \dot{\theta} \end{bmatrix} \tag{18}$$

$$y = x \tag{19}$$

The state space equations are:

$$\dot{x} = \frac{dx}{dt} \tag{20}$$

$$\ddot{x} = \frac{\frac{B_p \cdot \dot{\theta} \cdot \cos\theta}{l} - B_{eq} \cdot \dot{x} + f + m \cdot l \cdot \dot{\theta}^2 \cdot \sin\theta + m \cdot g \cdot \sin\theta \cdot \cos\theta}{M + m \cdot \left(1 - \cos^2\theta\right)} \tag{21}$$

$$\dot{\theta} = \frac{d\theta}{dt} \tag{22}$$

$$\ddot{\theta} = \frac{\cos\theta \cdot \left(-f + B_{eq} \cdot \dot{x} - m \cdot l \cdot \dot{\theta}^2 \cdot \sin\theta\right) - \left(M + m\right)\left(g \cdot \sin\theta + \frac{B_p \cdot \dot{\theta}}{m \cdot l}\right)}{M \cdot l + m \cdot l \cdot \left(1 - \cos^2\theta\right)} \tag{23}$$

OPEN LOOP SIMULATIONS

We simulate the system with the following parameters: l=0.3302 m; M=1.0731 kg; m=0.23 kg; r=0.00635 m; R=2.6 Ω; k=0.00767 N·m·A^{-1}; g=9.81 m·s^{-2}; B_{eq}=5.4 N·s·m^{-1} e B_p=0.0024 N·m·srad^{-1}. For validation, we simulate an open-loop step function response. The response of the trolley linear position x and sway angle θ are shown in Fig. 3 and Fig. 4.

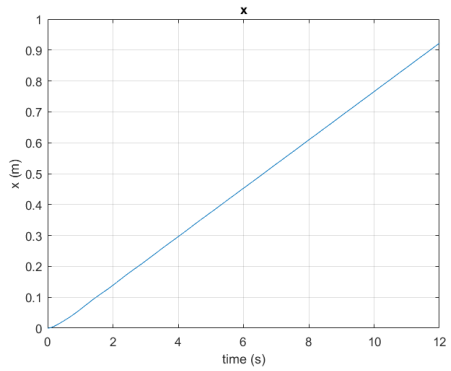

Figure 3 – Trolley linear position response due to step function input.

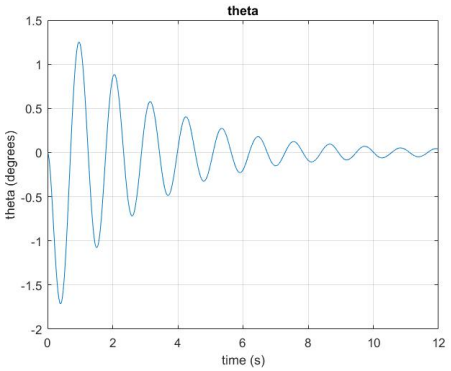

Figure 4 – Sway angle response due to step function input.

SLIDING MODE CONTROL

The controller purpose is to move the payload from an initial position to its destiny, minimizing the sway angle. It happens when the DC motor voltage source is controlled aiming to boost a force in the trolley, which is responsible for moving the payload. To manage it, we choose a sliding mode control, which is a robust non-linear control, capable of achieving stability and performance even when faced with structured or not structured model uncertainties (Slotine, 1991). To evaluate the synthetized control, is assumed that certain system parameters are not exactly known, even thought varying between known boundaries. Thus, R, k, B_{eq} and B_p are endowed with a ±10% uncertainty.

Sliding surface

We note that the control action acts in trolley linear position and sway angle, making the conventional sliding mode control synthesis harder, due to the fact that only one state variable is achieved. Therefore, we define a state variable z, which is a linear combination of x and θ. Then, we apply the sliding mode control to this variable (Qian and Yi, 2013), seeking that the trolley linear position and sway angle are both being taken into consideration in the control:

$$z = x + c \cdot \theta \tag{24}$$

where c is a positive constant, which determines the sway angle influence on the variable to be controlled. We derive the sliding surface as follows:

$$s = \dot{\tilde{z}} + \lambda \cdot \tilde{z} \tag{25}$$

$$\tilde{z} = z - z_d \tag{26}$$

where z_d is the setpoint value and λ is one of the sliding mode control tuning parameters.

Control law

Before applying the control system, it is interesting to rewrite the dynamic model as follows (Qian and Yi, 2013):

$$\dot{x} = \frac{dx}{dt} \tag{27}$$

$$\ddot{x} = g_1 + b_1 \cdot u \tag{28}$$

$$\dot{\theta} = \frac{d\theta}{dt} \tag{29}$$

$$\ddot{\theta} = g_2 + b_2 \cdot u \tag{30}$$

The sliding mode control law consists of two parts (Utkin, 1992): the equivalent control law $\hat{u}$ and the switching control law u_c, which can be calculated by deriving Eq. (25) and applying the feedback linearization technique:

$$u = \hat{u} + u_c \tag{31}$$

$$\hat{u} = \frac{-\lambda \cdot \dot{\tilde{z}} - \hat{g}_1 - c \cdot \hat{g}_2 + \ddot{z}_d}{b_1 + c \cdot b_2} \tag{32}$$

$$u_c = \frac{-K \cdot \mathrm{sgn}\left(s\right)}{b_1 + c \cdot b_2} \tag{33}$$

where $\hat{g}_1$ is an estimate of g_1, $\hat{g}_2$ is an estimate of g_2, which we calculate by the simple mean between the maximum and the minimum values of g_1 and g_2. We define the sliding condition by the following equation (Slotine, 1991):

$$\frac{1}{2} \cdot \frac{ds^2}{d^2t} \leq -\eta \cdot s \tag{34}$$

where η is one of sliding mode control tuning parameters and must be a strictly positive constant (Slotine, 1991). The sliding mode control gain K must be large enough to always satisfy the sliding condition (Slotine, 1991). Then:

$$K = \eta + G \tag{35}$$

where G is the function that limits the values of $\hat{g}_1$ and $\hat{g}_2$. We calculate G developing Eq. (32), as follows:

$$G = \max\left|g_1 - \hat{g}_1 + c\cdot\left(g_2 - \hat{g}_2\right)\right| \tag{36}$$

CLOSED LOOP SIMULATIONS

To perform the designated tasks efficiently, it is necessary that the overhead crane meets the following performance parameters: t_s=10 s; M_p=0% and $|\Delta\theta|$=±2°, where t_s is the trolley settling time (2% criteria), M_p is the overshoot and $|\Delta\theta|$ is the sway angle maximum variation. The controller tuning parameters are: λ=0.8 and η=0.4. The initial conditions vector is null and the setpoint vector is x_d=[0 1 0 0]^T, which implies in z_d=[0 1 0 0]^T. Initially, we analyze the case with c=0, purposing to observe how the system behaves when the sliding mode control only takes into consideration the trolley linear position. The trolley linear position x, the sway angle θ and the sliding surface responses are shown in Fig. 5, Fig. 6 and Fig. 7.

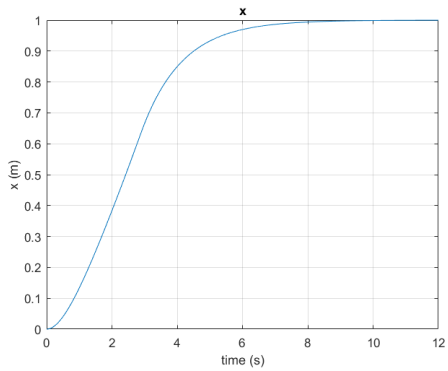

Figure 5 – Trolley linear position response due to z_d=[0 1 0 0]^T.

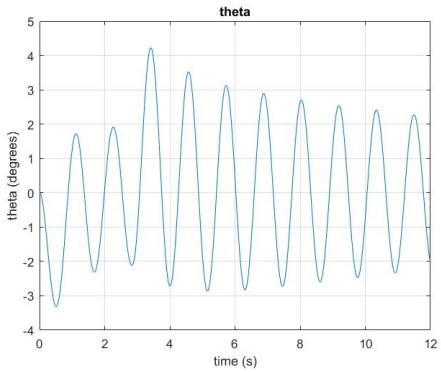

Figure 6 – Sway angle response due to z_d=[0 1 0 0]^T.

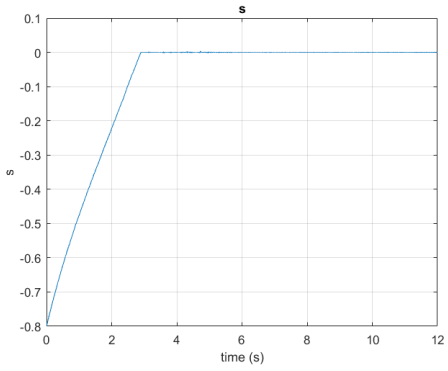

Figure 7 – Sliding surface response due to z_d=[0 1 0 0]^T.

ALTERNATIVE APPROACH

We note that the sway angle, besides oscillating too much, does not reaches the setpoint at the same time as the trolley linear position does. Another issue detected observing the Fig. 8 is the chattering phenomenon. The control

action switches several times, leading to high control activity, which may lead to the wear and tear of the overhead crane elements (Slotine, 1991).

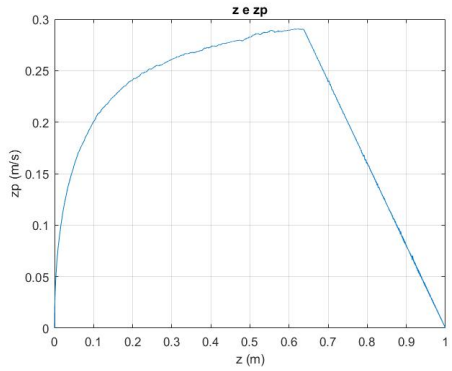

Figure 8 – Trolley linear velocity response by trolley linear position due to $z_d=[0\ 1\ 0\ 0]^T$.

To face those issues, we propose another approach, dodging the problems and improving the controller performance.

Saturation

To avoid chattering, we replace the on-off switching control law saturation as derived in Eq. (33) (Slotine, 1991) by:

$$u_c = \frac{-K \cdot sat\left(\frac{s}{\varphi}\right)}{b_1 + c \cdot b_2} \tag{37}$$

where φ is the boundary layer thickness.

Variable setpoint

Analyzing how the setpoint variation affects the system response, it is noted that $z_d=[0\ 1\ 0\ 0]^T$ for $t \geq 0$ leads to highly oscillatory sway angle behavior. This event happens because in the beginning of the control action, the setpoint already assumes it's final value. So, we smoothly change the setpoint as time varies, reducing the oscillation and sway angle settling time, penalizing the trolley setting time. The next simulations uses the following controller parameters: $\varphi=0.5$; $z_d=[0\ 1\text{-}e^{-t}\ 0\ 0)]^T$. Fig. 9 and Fig. 10 shows respectively the trolley linear position response and the sway angle response.

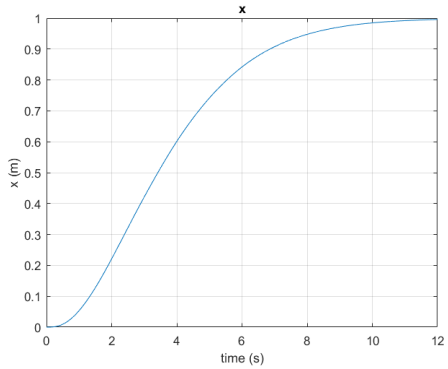

Figure 9 – Trolley linear position response – first alternative approach.

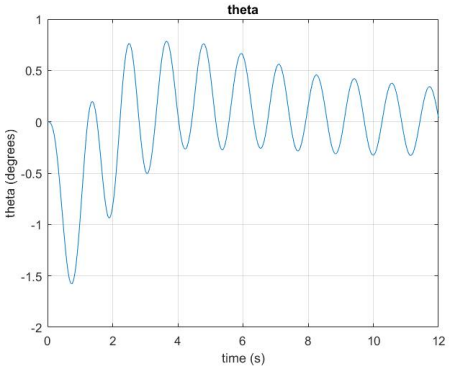

Figure 10 – Sway angle response – first alternative approach.

We note that the sway angle oscillation is diminished, but still oscillates too much, evidencing that the regular sliding mode control associated with saturation and variable setpoint is insufficient to solve all adversities. So, another alternative approach is proposed.

Combining sliding mode control

To take the trolley linear position and sway angle both into consideration, we use a combined sliding mode control as follows. After a few iterations, always taking into consideration the commitment relationship already mentioned between the performance parameters, the optimum controller parameters are: φ=0.5; c=0.33; z_d=[0 1-e^{-t} 0 0)]$^{\mathbf{T}}$. Fig. 11, Fig. 12, Fig. 13 and Fig. 14 shows respectively the trolley linear position response, the sway angle response, the sliding surface response, and the trolley linear velocity response by trolley linear position. The dotted line and the full line represent the optimized system and the non-optimized system responses, respectively.

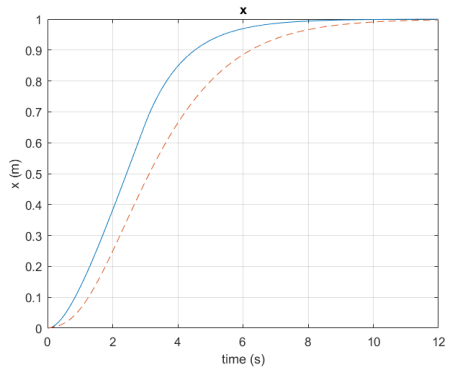

Figure 11 – Trolley linear position response – comparison between the controllers.

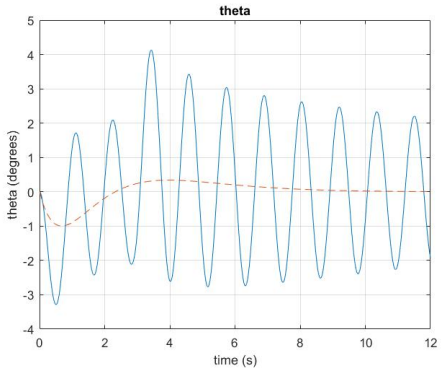

Figure 12 – Sway angle response – comparison between the controllers.

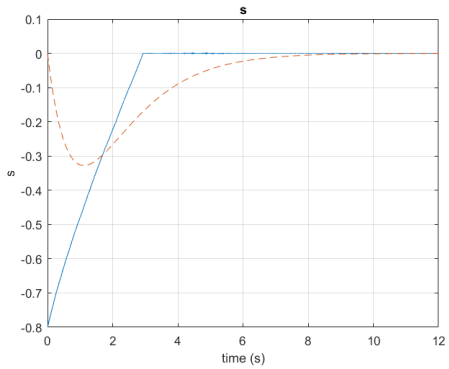

Figure 13 – Sliding surface response – comparison between the controllers.

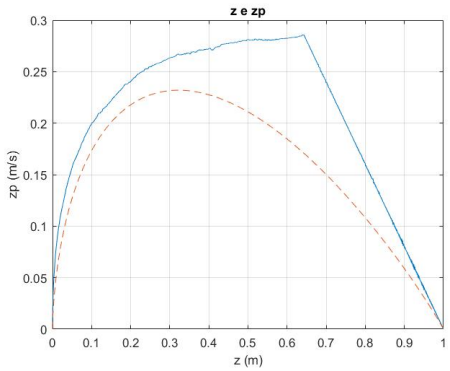

Figure 14 – Trolley linear velocity response by trolley linear position – comparison between the controllers.

STABILITY ANALYSIS

Using the Lyapunov stability criterion and choosing s as the Lyapunov function, it can proved that z is asymptotically stable when $t \rightarrow \infty$. However, the convergence of the states is not assured, being this issue solved by the damping force acting upon the sway angle.

ANALYSIS of RESULTS

Observing Fig. 11 and Fig. 12, we note that t_s=10 s; M_p=0% and $|\Delta\theta|$=±2°. Hence, all performance requirements formerly defined were achieved. Analyzing Fig. 14, it is shown that the use of saturation in control action eliminates the chattering phenomenon, yet worsening the controller performance, which is denoted by the 0.14 mm steady state error, besides rendering to a slower trolley response. From Fig. 11 and 12, we note that the combined sliding mode control leads to a sway angle maximum amplitude reduction and setpoint time closer to the trolley linear position. The setpoint variation in time, which we shaped as a first order linear system with unitary time constant response due to step function input, leaded to a big sway angle oscillation frequency reduction, penalizing the trolley linear position settling time, since the control action acting upon the system develops in a smother way, because the setpoint increases over time.

CONCLUSIONS

The goal of synthetize a robust non-linear controller that aims the sway angle oscillation and amplitude suppression, penalizing the payload mass travel time and trolley accuracy was successfully achieved, since all performance parameters were granted, even when the system is subjected by parametric uncertainties. The addressed problem also illustrates the sub actuated systems control main difficulties, evidencing that convention control techniques are not sufficient in order to achieve success in the goals initially outlined for this article.

REFERENCES

Bolton, W., 2004, Mechatronics: Electronic Control Systems in Mechanical and Electrical Engineering, Pearson Education, Harlow.

França L. N. F. and Matsumara A. Z., 2012, Mecânica Geral, Edgard Blucher, São Paulo.

Friedland B., 1986, Control System Design: An Introduction to Space-State Methods, McGraw-Hill, New York.

Iles S., Kolonic F., Matsuko J., 2011, Linear Matrix Inequalities Based H1 Control of Gantry Crane Using Tensor Product Transformation, Proceedings 18th International Conference on Process Control, pp. 92-99.

Jafari J., Ghazal M. and Nazemizadeh M., 2014, A LQR Optimal Method to Control the Position of an Overhead Crane, International Journal of Robotics and Automation, Vol. 3, No.4, pp. 252-258.

Nazemizadeh, M., 2013, A PID Tuning Method for Tracking Control of an Underactuated Gantry Crane, Universal Journal of Engineering Mechanics 1, pp. 45-49.

Park, H., Chwa, D. and Hong K., 2007, A Feedback Linearization Control of Container Cranes: Varying Rope Length, International Journal of Control, Automation, and Systems, Vol. 5, No.4, pp. 379-387.

Qian D. and Yi J., 2013, Design of Combining Sliding Mode Controller for Overhead Crane Systems, International Journal of Control and Automation, Vol. 6, No.1, pp. 131-140.

Slotine J. and Li W., 1991, Applied Nonlinear Control, Prentice-Hall, New Jersey.

Utkin V., 1992, Sliding Modes in Control and Optimization, Springer-Verlag Berlin, Heidelberg.

RESPONSIBILITY NOTICE

The authors are the only responsible for the material included in this paper.